

UNCLASSIFIED



**Australian Government**  
**Department of Defence**  
Defence Science and  
Technology Organisation

# Residual Stress Development in Explosive-Bonded Bi-Metal Composite Materials

*C. Choi<sup>1</sup>, V. Luzin<sup>2</sup>, M. Callaghan<sup>3</sup>, N. Lane<sup>4</sup> and B. Dixon<sup>1</sup>*

<sup>1</sup> **Land Division**

Defence Science and Technology Organisation

<sup>2</sup> Australian Nuclear Science and Technology Organisation

<sup>3</sup> The University of Manchester

<sup>4</sup> The University of Wollongong

DSTO-TR-2945

## ABSTRACT

One of the main obstacles of applying explosive welding for improved mechanical and corrosion properties of bimetal composite materials is the potential for a residual stress contour to exist at the interface to be bonded, which could be detrimental to the life of the vehicle. Therefore it is important to study the distribution of the residual stress over the welded material, especially at the interface area. A range of varieties of steel plate materials, possessing different chemistries, mechanical properties and thicknesses, were explosive welded to produce bi-metallic plates. Neutron diffraction experiments were undertaken to investigate the residual stress development in these bi-metallic plates. The characteristic residual stress formations in the plate systems were observed to be influenced by microstructural evolution at the weld interface as well as the mechanical properties and thicknesses of the original plate materials. It was found that explosive welded plates have tensile residual stresses in both the longitudinal and transverse direction at the interface. The level of these stresses is close to yield.

## RELEASE LIMITATION

*Approved for public release*

UNCLASSIFIED

UNCLASSIFIED

*Published by*

*Land Division*

*DSTO Defence Science and Technology Organisation*

*506 Lorimer St*

*Fishermans Bend, Victoria 3207 Australia*

*Telephone: 1300 333 362*

*Fax: (03) 9626 7999*

*© Commonwealth of Australia 2014*

*AR-015-876*

*March 2014*

UNCLASSIFIED

**UNCLASSIFIED**

# Residual Stress Development in Explosive-Bonded Bi-Metallic Composite Materials

## Executive Summary

One of the main obstacles of applying explosive welding for improved mechanical and corrosion properties of bimetal composite materials is the potential for a residual stress contour to exist at the interface to be bonded, which could be detrimental to the life of the vehicle. Therefore it is important to study the distribution of the residual stress over the welded material, especially at the interface area.

A variety of steel plate materials, possessing different chemistries, mechanical properties and thicknesses, were explosive welded to produce bi-metallic plates.

Neutron residual stress measurements was conducted to measure the residual stresses along the through-thickness direction of the bonded joints, for both the longitudinal and transverse directions. The trends shown in the development of longitudinal and transverse residual stresses were similar in each joint, regardless of materials combinations and thicknesses. Tensile residual stresses were observed to be greatest at the weld interface, with compressive residual stresses produced in the unaffected base metal. It was found that steels possessing high toughness and ductility produced residual stresses that exceeded the yield strengths of these materials, however, the yield strengths were less than those of steels which have higher strength.

The quantification of residual stress development in these systems may be used together with other analytical and mechanical techniques, to inform potential armour design based on metal-metal composite plates produced through the explosive welding process.

**UNCLASSIFIED**

UNCLASSIFIED

*This page is intentionally blank*

UNCLASSIFIED

## Authors

### **Chang-Ho Choi**

Defence Science and Technology Organisation

Chang-Ho Choi obtained a Masters degree in Materials Science at the University of Oregon and undertook PhD study at the University of Illinois and later at the University of New South Wales, where he received a PhD with a thesis on superconductors. He has been employed as a materials scientist at DSTO Maritime Platforms Division since 1998. During the period 1998 to 2006, he worked with the metallurgy section. From 2006 to 2009, he worked in the biology section and from 2009 onward, in the Armour Mechanics and Vehicle Survivability group of Land Division.

---

### **Vladimir Luzin**

Australian Nuclear Science and Technology Organisation

Dr Vladimir Luzin is responsible for the residual stress diffractometer at the OPAL research reactor, since joining ANSTO in 2006. His expertise covers neutron diffraction for studies of residual stresses and textures in various industrial components and materials. His experience is gained in several international neutron research facilities JINR (pulsed reactor IBR-2), GKSS (neutron facility FRG-1), NIST (research reactor NBSR) and ANSTO (OPAL research reactor).

---

### **Mark Callaghan**

The University of Manchester

Mark Callaghan undertook his PhD at ANSTO, researching high temperature fatigue behaviour and modelling of ferritic pressure vessel steel, for which he was awarded the degree at the University of Technology, Sydney in 2009. He joined the University of Wollongong in 2008 as a Research Fellow, where he undertook research into armour and high strength steels subjected to static and dynamic loadings, weldability and welding metallurgy of these materials as a function of welding processes and simulations. In 2012, Mark was appointed as Research Associate at The University of Manchester, researching thick-walled corrosion resistant materials for high-temperature high-pressure service.

---

**Nathan Lane**

The University of Wollongong

Nathan Lane is currently undertaking a PhD, researching the toughness and weldability of high strength steels for naval surface ship applications through The University of Wollongong and previously on secondment to DSTO Maritime Platforms Division. He joined The University of Wollongong in 2012 as an Associate Research Fellow, investigating the toughness and weldability of high strength steels for submarine construction and armour steels.

---

**Brian Dixon**

Defence Science and Technology Organisation

Brian Dixon is a metallurgy scientist in the Maritime Platforms Division of Defence Science and Technology Organisation. He has been employed at DSTO since 1978, undertaking experimental development and fundamental studies into weld metal solidification cracking in steels and stainless steels. He has also undertaken extensive work on improving the weld zone toughness of high strength steels. During 1989 and 1990 Brian worked at Kockums Laboratory in Sweden as part of DSTO's contribution to the submarine project. Since 2001, Brian has worked in a number of developmental positions, including Director, Program Office (Maritime), STCC for M1 and M6 and S&T Adviser for JP 2048. He is currently head of the Armour Mechanics and Vehicle Survivability Group.

---

# Contents

1. INTRODUCTION.....	1
2. EXPERIMENTAL .....	3
2.1 Materials and Explosive Welding Methodology .....	3
2.2 The Principles of Neutron Diffraction for Stress Measurement .....	5
2.3 Neutron Diffraction Experiments.....	7
3. RESULTS AND DISCUSSIONS.....	8
3.1 Composite Plate Bonding and Interface Characteristics .....	8
3.2 Residual Stress Development in Composite Plates .....	13
4. CONCLUSIONS.....	18
5. ACKNOWLEDGEMENTS .....	18
6. REFERENCES .....	19

UNCLASSIFIED

*This page is intentionally blank*

UNCLASSIFIED



# 1. Introduction

Armour steels are generally categorised as high strength steels, with their microstructures and resultant properties tailored to defeating both ballistic and blast threats. Since World War II, numerous steels have been researched and introduced to protect armoured vehicles. These include rolled homogeneous armour (RHA), high hardness armour (HHA), high toughness armour (HTA) and ultra-high hardness armour (UHA). These steels rely on hard microstructural phases (notably martensite) to attain their strength and hardness, but with an inherent sacrifice in toughness and ductility. Traditionally, it has been considered that obtaining strength, toughness and ductility simultaneously in a material is difficult, because the properties are essentially mutually exclusive.

In considering an optimised protective armoured system, strength and hardness are vital to protect against and defeat impact events from blast, as well as provide structural integrity for armoured vehicles. However, toughness and ductility are required by the material to absorb kinetic energy of blast waves, hence avoiding catastrophic failure. Ideally, the protective system requires all these properties in concert to provide optimum survivability. Obtaining these properties with conventional monolithic steel armour is exceedingly difficult. One method in achieving these properties is to join steel possessing different properties such as high strength and hardness, with another steel possessing high toughness and ductility, thus creating a composite plate with good all-round mechanical properties as shown in Figure 1. In order to achieve this, bi-metallic plates require a continuous join between the surfaces of both plates, which is not attainable through typical fusion welding techniques. Therefore, explosive welding (EW), utilising an impact of a flyer plate with that of a stationary base plate (hence inducing a solid-state continuous bonded joint) presents a convenient method to tailor either similar or dissimilar steels to achieve these properties within one system. Further, this process can be used to conveniently join similar or dissimilar steels, which may not be able to be joined by fusion processes.

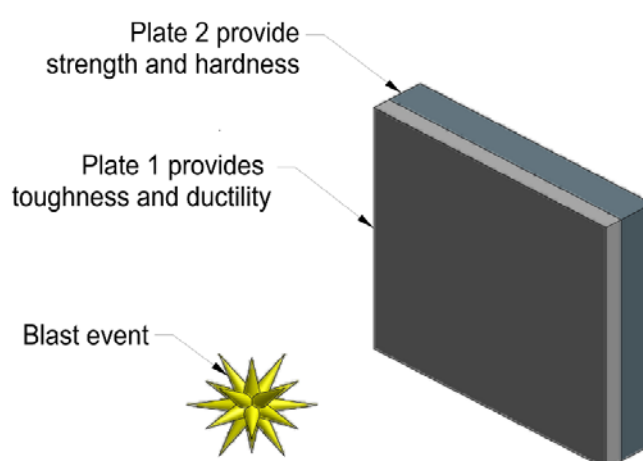


Figure 1: Composite plate configuration to protect against a blast event, with plate 1 providing toughness and ductility properties and plate 2 providing strength and hardness properties.

In optimised bi-metallic protective systems, one plate provides strength and hardness, whilst the other plate reinforces toughness and ductility of the system. The configuration of the two plates depends on the overall purpose of the protective system.

The metallurgical bond produced through EW is of particular importance in these joints, due to complex metallurgical interactions that occur. These have been described in a previous study [1] and involve localised severe plastic deformation, high strain rate deformation of base material through shock loading, areas of intense localised heating and subsequent phase transformations. Further, residual stresses are important within potential composite systems, because these may not only provide ballistic/blast protection, but also improve structural integrity. However, one of the main issues with applying explosive bonding for improving mechanical and metallurgical properties of the materials may be residual stress contour on the interface to be bonded, as this may be detrimental to the life of the vehicles. For this reason, it is important to study the distribution of the residual stress over the blast material, especially the interface area.

Residual stresses exist within a component or assembly in the absence of any externally applied load, but usually as a result of thermo-mechanical treatment such as forming, welding, joining, machining, heat treatment, abrasion, peening and other simple processes of fabrication [2, 3]. The residual stresses may also originate from shape misfits between different regions of a component. The basic cause of these misfits is non-uniform plastic deformation. The same effect can occur even under uniform plastic deformation, such as in conditions where temperature gradients are responsible for different accumulated plastic deformation in parts of a component. In practice, it is important to determine whether the local parts of interest suffer compressive or tensile stress, because depending on the status of stress, premature failure modes can occur on the assembled part. It is well known that the compressive residual stress on the surface of a component is beneficial in reducing the likelihood of failure in the particular region of a component. It may even increase the component's resistance to an externally applied load.

Residual stresses have been shown to influence structural integrity, including fatigue strength and endurance-life [4, 5]. However, information detailing residual stresses produced by the EW process is lacking with a single work providing some theoretical estimates [6] and a few publications with experimental results [2, 3]. The ability to quantify residual stresses would thus be a worthy goal to inform potential armour design based on bi-metallic plates produced through the EW process.

In this report, a series of 8 types of steel plate materials possessing different chemistries, mechanical properties and thicknesses, were joined through the EW process. Neutron diffraction experiments were then carried out at the residual stress diffractometer Kowari at OPAL research reactor at Australian Nuclear Science and Technology Organisation (ANSTO) (Lucas Heights, Australia), in order to characterise the residual stress development through the thickness of the composite plates as a function of both EW process and steel plate combinations.

## 2. Experimental

### 2.1 Materials and Explosive Welding Methodology

Eight explosive welding experiments were undertaken in this study, using three flyer plate materials including TWin Induced Plasticity (TWIP) steel, Grade 350 mild steel and superaustenitic steel and three alternative bottom plate materials, TWIP steel, Grade 350 mild steel, and high strength, high hardness 'HARD' steel. The plate combinations, charge weight, charge thickness and angle of flyer plate are given in Table 1. All steels possessed different chemistry, heat-treatment and hence mechanical properties and the differences in mechanical properties are shown in Table 2.

Table 1: Plate combinations and charge weights used for explosive bonding.

No	Plate Combination (mm)	Charge Weight (kg)	Charge Thickness (mm)	Angle (°)
1	TWIP (8.5) + TWIP (2.6)	0.56	11.9	10
2	G350(8.5) + TWIP (2.6)	0.56	11.9	10
3	TWIP (2.6) + TWIP (8.5)	0.18	3.6	10
4	TWIP (2.6) + G350 (8.5)	0.18	3.6	10
5	G350 (8.5) + G350 (8.5)	0.56	11.9	10
6	TWIP (8.5) + TWIP (8.5)	0.56	11.9	10
7	TWIP (2.6) + TWIP (2.6)	0.18	3.6	10
8	SA <sup>1</sup> (8.5) + HARD <sup>2</sup> (4.3)	0.56	11.9	10

Table 2: Typical mechanical properties of superaustenitic steel, TWIP steel and HARD steels.

Material	Yield strength (MPa)	Ultimate tensile strength (MPa)	Elongation (%)
TWIP steel	640	780	60
Grade 350 steel	350	430	>15
HARD steel	1150	1450	13
Superaustenitic steel	430	700-950	>35

These plates were water-jet cut to dimensions of 180 mm × 180 mm. The explosive charge was contained in wooden boxes with dimension of 180 mm × 180 mm × 100 mm. The configuration for explosive bonding is shown in Figure 2.

<sup>1</sup> SA: Superaustenitic steel.

<sup>2</sup> The brand name of HARD steel is protected.

This shows the details of the plate preparation used for explosive bonding tests. The computation of the charge thickness for the flyer plate was followed by the Gurney equation [7]

$$\frac{M}{C} = \frac{\rho_m \cdot t_m}{\rho_e \cdot t_e} \quad (1)$$

With the ratio of mass of the fragments ( $M$ ) and the mass of the explosive ( $C$ ) fixed as constant,  $\rho_m$  = plate density ( $\text{kg}/\text{m}^3$ ),  $t_m$  = plate thickness (m),  $\rho_e$  = explosive density ( $\text{kg}/\text{m}^3$ ), and  $t_e$  = explosive thickness (m), under the assumption that the chemical energy of the explosive was transformed into kinetic energy of the explosive products and metal fragments.

The flyer plate was placed on the top of the bottom plate for each test with  $10^\circ$  angle ( $\beta$ ) between the two plates. Figure 2 shows the schematic diagram of the material preparation for the explosive bonding experiments.

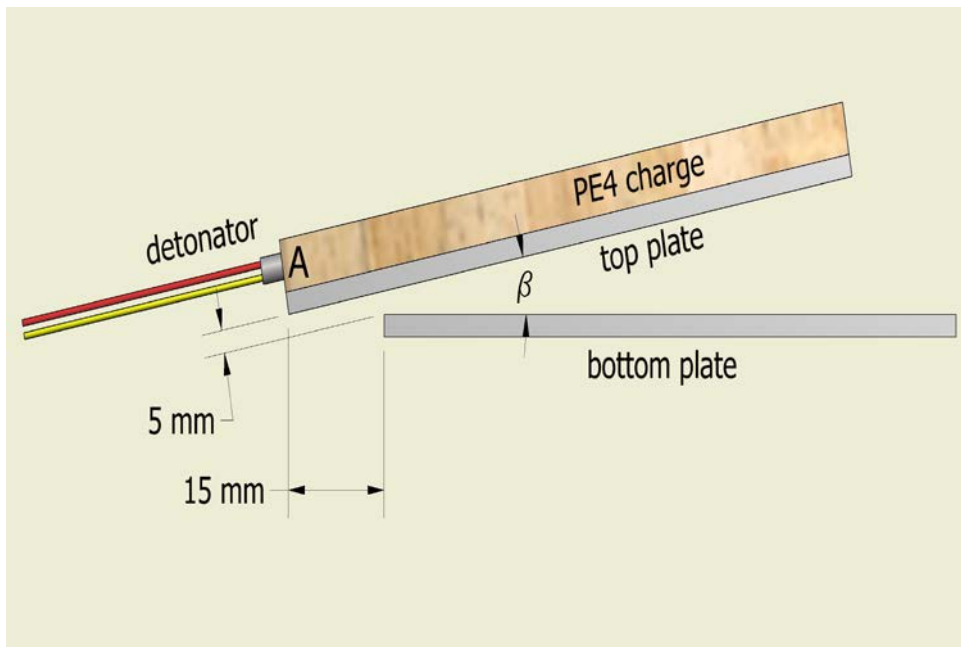


Figure 2: A schematic (not to scale) of the configuration and position of the flyer (top) and bottom plates adapted from [1], together with PE4 charge.  $\beta$  represents the angle between the plates (fixed  $10^\circ$  for this project).

As shown in Figure 2, the flyer plate was located 15 mm beyond the left hand edge of the bottom plate. This was done to optimise the jetting action developed between the two plates. The region marked 'A' indicates the location of the detonator, which was inserted into a drilled hole in the explosive. The apparatus was located on a 20 mm rubber mattress for shock absorbing purposes.

## 2.2 The Principles of Neutron Diffraction for Stress Measurement

Neutrons are elementary particles with approximately the mass of a proton but no electric charge. Due to this charge neutrality they can penetrate deep into material and are typically about a thousand times more penetrating than X-rays. In nuclear research reactors, fast neutrons produced in fission nuclear reactions are slowed down by specially designed moderators, so that they possess a wavelength similar to the lattice spacing of typical engineering materials (metals, ceramics), which makes them very suitable for strain measurement using neutron diffraction.

Neutron diffraction is a measurement technique which closely parallels X-ray diffraction in methodology and analytical procedure. The geometrical principle of diffraction is shown in Figure 3, illustrating the diffracted planes and wave vectors, as well as scattering vector. Similar to the X-ray stress measurement technique, neutrons also can be used for stress measurements. However, due to the high penetration of neutrons, the residual stresses can be measured non-destructively within the interior of components in small test volumes (called gauge volume, can be as small as  $0.5 \times 0.5 \times 0.5 \text{ mm}^3$ ) and in thick specimens (up to 50-70 mm in steel) using neutron diffraction.

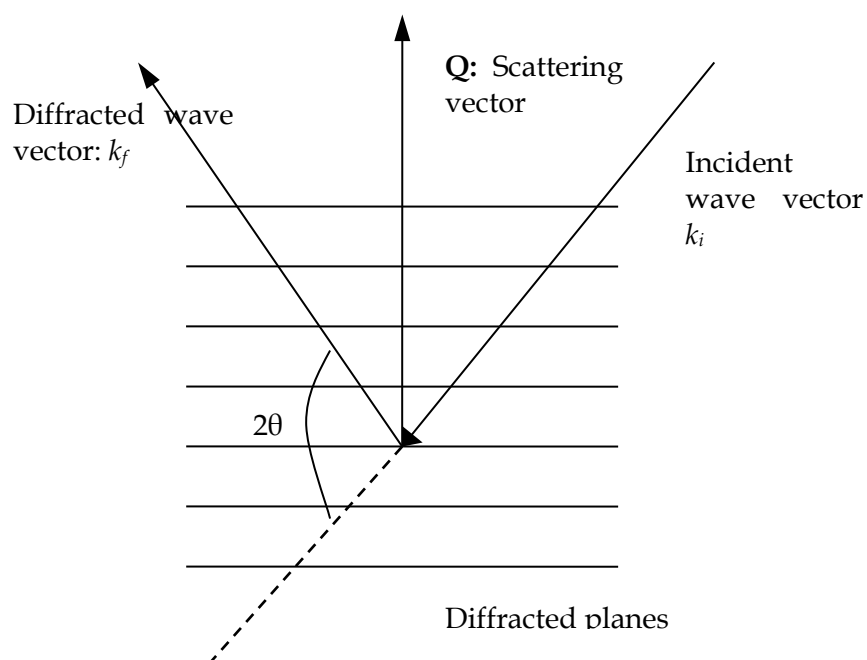


Figure 3: The principles of neutron diffraction.

When a beam of neutrons is passed through a polycrystalline material, diffraction occurs and diffraction peak appears according to Bragg's law, given by equation (2):

$$\lambda = 2d_{hkl} \sin \theta_{hkl} \quad (2)$$

where  $\lambda$  is the wavelength of the radiation used,  $\theta_{hkl}$  is the Bragg angle for crystallographic planes,  $hkl$ , having interplanar spacing,  $d_{hkl}$ .

Under an applied tensile or compressive stress, the lattice spacing in individual crystalline grains expands or contracts. This causes a relative change in the lattice spacing, or strain. At constant wavelength, this change can be detected as a shift in position of the diffraction peaks. From Bragg's law, the strain is given by equation (3). The 'naught' values in equations (3) and (4),  $d_0$  and  $\theta_0$ , refer to the reference stress-free sample.

$$\varepsilon_{hkl} = \frac{d_{hkl} - d_0}{d_0} = \frac{d_{hkl}}{d_0} - 1 \quad (3)$$

$$\varepsilon = \frac{\sin \theta_0}{\sin \theta} - 1 \quad (4)$$

The strain uncertainty,  $\Delta\varepsilon$ , measurement can then be calculated by equation (5):

$$\Delta\varepsilon = \frac{1}{d_0} \sqrt{(\Delta d)^2 + (\Delta d_0)^2} \quad (5)$$

If measurements are done in three principal directions of a three dimensional solid, then the strains ( $\varepsilon_{xx}$ ,  $\varepsilon_{yy}$ ,  $\varepsilon_{zz}$ ) can be calculated from the stress tensor components ( $\sigma_{xx}$ ,  $\sigma_{yy}$ ,  $\sigma_{zz}$ ) using elasticity theory for elastically isotropic solid. It gives equation (6):

$$\begin{aligned} \sigma_{xx} &= \frac{E}{(1+\nu)(1-2\nu)} \left[ (1-\nu)\varepsilon_{xx} + \nu(\varepsilon_{yy} + \varepsilon_{zz}) \right] \\ \sigma_{yy} &= \frac{E}{(1+\nu)(1-2\nu)} \left[ (1-\nu)\varepsilon_{yy} + \nu(\varepsilon_{xx} + \varepsilon_{zz}) \right] \\ \sigma_{zz} &= \frac{E}{(1+\nu)(1-2\nu)} \left[ (1-\nu)\varepsilon_{zz} + \nu(\varepsilon_{xx} + \varepsilon_{yy}) \right] \end{aligned} \quad (6)$$

From (6)  $E \equiv E_{hkl}$  is Young's modulus, and  $\nu = \nu_{hkl}$  is Poisson's ratio. Because of elastic anisotropy of the material, they are hkl sensitive and should be calculated (or evaluated by other means) for the specific hkl reflection used in the neutron measurements. The uncertainties of the stress components are defined as:

$$\begin{aligned} \Delta\sigma_{xx} &= \frac{E}{(1+\nu)(1-2\nu)} \sqrt{\Delta\varepsilon_{xx}^2 + \nu^2 (\Delta\varepsilon_{yy}^2 + \Delta\varepsilon_{zz}^2)} \\ \Delta\sigma_{yy} &= \frac{E}{(1+\nu)(1-2\nu)} \sqrt{\Delta\varepsilon_{yy}^2 + \nu^2 (\Delta\varepsilon_{xx}^2 + \Delta\varepsilon_{zz}^2)} \\ \Delta\sigma_{zz} &= \frac{E}{(1+\nu)(1-2\nu)} \sqrt{\Delta\varepsilon_{zz}^2 + \nu^2 (\Delta\varepsilon_{xx}^2 + \Delta\varepsilon_{yy}^2)} \end{aligned} \quad (7)$$

The geometry of the samples allows significant simplification of the stress analysis, because the thickness of the plates is much smaller than the other two dimensions. The plane stress state condition,  $\sigma_{zz} = 0$ , can be used as a very accurate approximation. (It was also proved experimentally, see Results.) In this case equations (6) can be reduced to Eq (8):

$$\begin{aligned}\sigma_{xx} &= \frac{E}{(1+\nu)(1-\nu)} \left[ \varepsilon_{xx} + \nu \varepsilon_{yy} \right] \\ \sigma_{yy} &= \frac{E}{(1+\nu)(1-\nu)} \left[ \varepsilon_{yy} + \nu \varepsilon_{xx} \right]\end{aligned}\quad (8)$$

### 2.3 Neutron Diffraction Experiments

The neutron strain scanning was carried out on the residual stress diffractometer Kowari at OPAL research reactor at ANSTO (Lucas Height, Australia). Scanning was done with high spatial resolution of 0.5 mm in the through-thickness dimension, using a  $0.5 \times 0.5 \times 20$  mm<sup>3</sup> gauge volume with the longest dimension being the in-plane direction. This high resolution was necessary to resolve stresses in the thinnest plates with thickness of just 2 mm and in anticipation of strong stress gradients especially in the interface area. At the same time this gauge volume enabled us to make multiple through thickness measurements (usually with steps 0.4-0.6 mm) in many samples within an allocated time.

Since these experiments involving two different crystal structures, ferritic  $\alpha$ Fe and austenitic  $\gamma$ Fe steels, two different reflections were used,  $\alpha$ Fe(211) and  $\gamma$ Fe(311), but always in close-to-90° geometry (Bragg angle for this reflection at  $2\theta = 90^\circ$ ) for the best localisation of the gauge volume. To achieve this, a monochromatic neutron beam from Si(400) reflection of Si monochromators was put at two take-off angles of 76° and 69° to provide the neutron wavelength of 1.67 Å and 1.54 Å for the reflections  $\alpha$ Fe(211) and  $\gamma$ Fe(311) correspondingly. Since plate thicknesses varied from 2 mm to 19 mm, the measurement time was also adjusted to provide a target strain accuracy of approximately 100 microstrain. When such accuracy is achieved, this results in a stress uncertainty of 20 MPa. Three principal directions, two mutually perpendicular in-plane and normal, were measured for all samples enabling in plane stress reconstruction assuming zero plane stress condition (the stress in the through-thickness condition is zero). In the stress reconstruction the following hkl-dependent elastic constants were used to reflect elastic anisotropy of the materials:  $E_{211} = 224.6$  GPa and  $\nu_{211} = 0.284$  for  $\alpha$ Fe(211) reflection and  $E_{311} = 203.3$  GPa and  $\nu_{311} = 0.304$  for  $\gamma$ Fe(311).

### 3. Results and Discussions

#### 3.1 Composite Plate Bonding and Interface Characteristics

Figure 4 shows the side view of the explosive-bonded composite plates, possessing similar and dissimilar material combinations as well as thicknesses. Most plates are observed to have some deformation bowing, which was oriented in the same direction as that of the blast impact. All plates were found to have formed solid joints at the interface, including the joint shown in Figure 4g where some disbonding occurred. This plate possessed materials with the greatest hardness, however, detonation velocity of the explosive may also have an influence. This matter will be discussed in another paper.

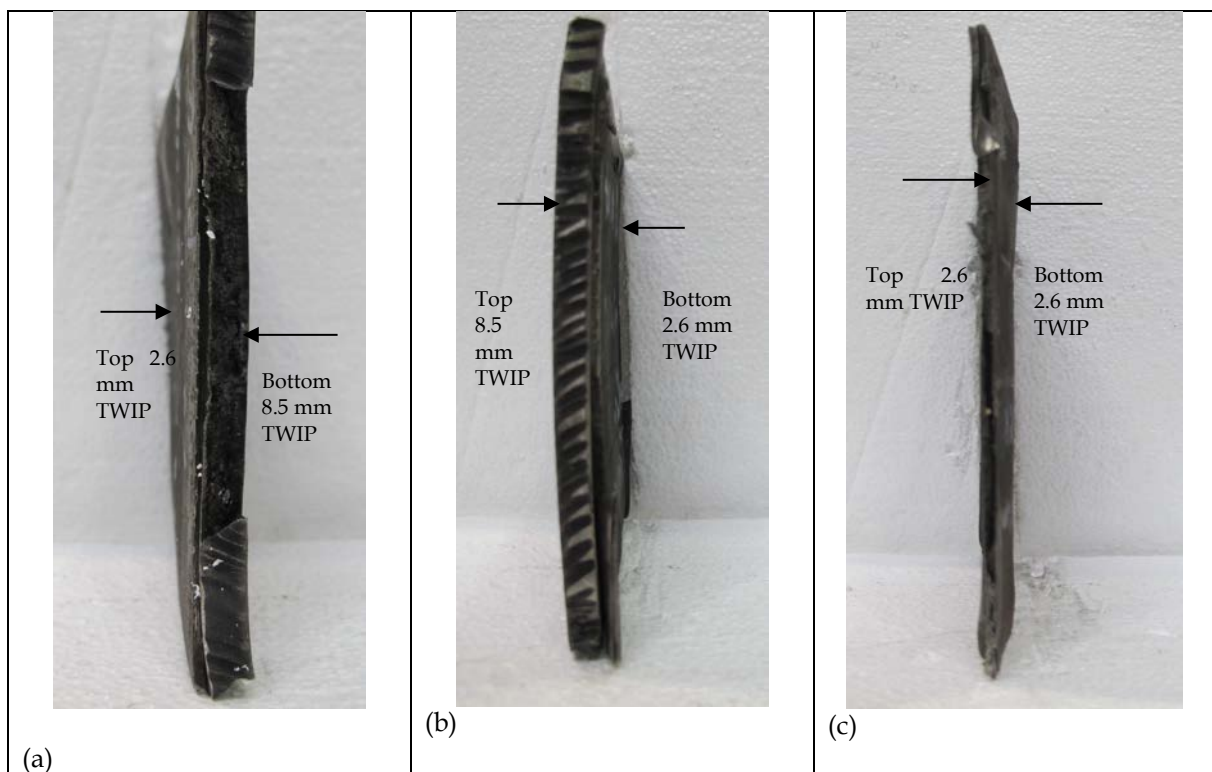


Figure 4: The side views of the explosive bonded plates (continued next page)



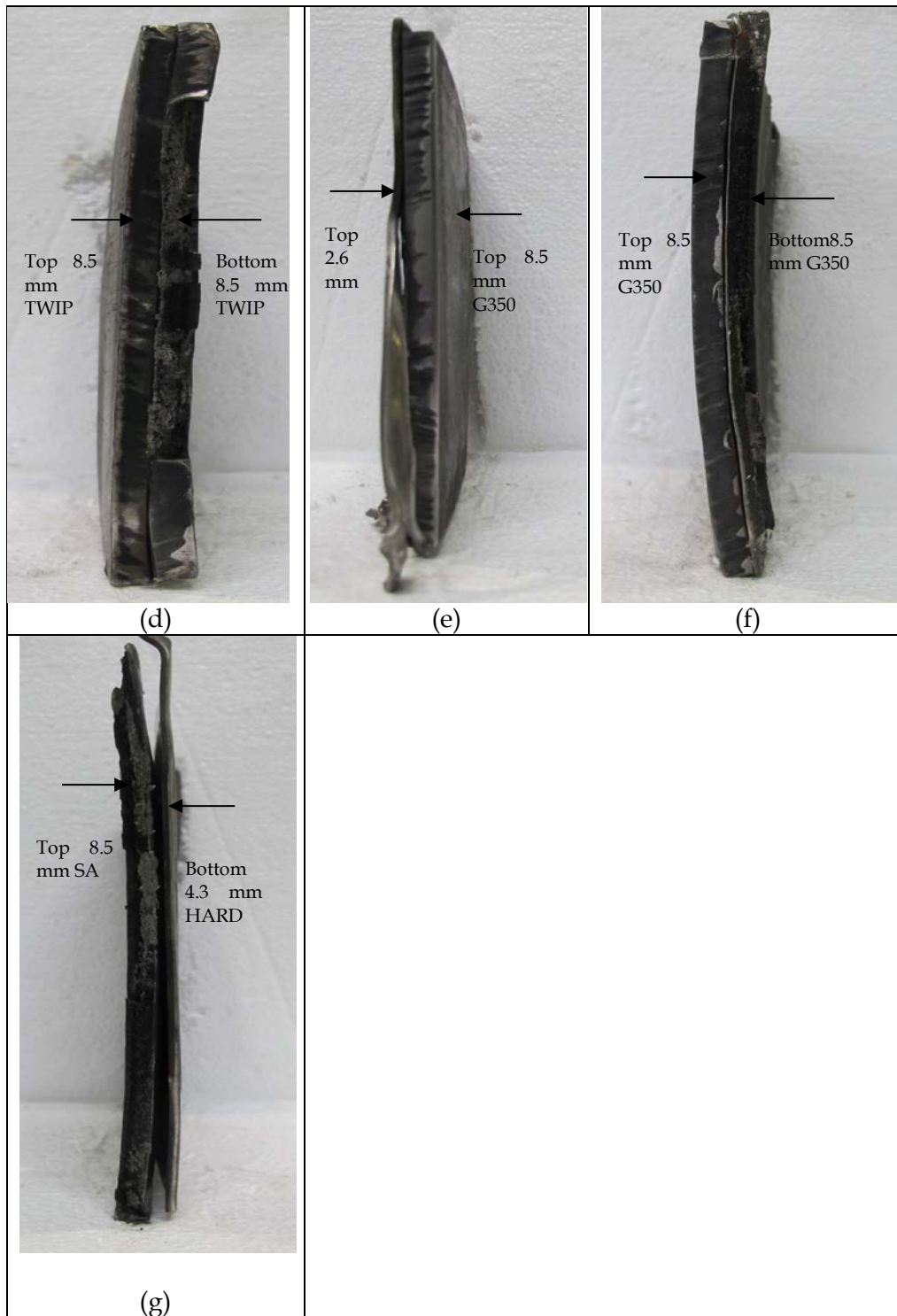


Figure 4 (continued)

In Figures 5 to 12, the typical wave-interface morphology produced during the EW process is observed for each plate combination through optical micrographs. This was achieved using standard practices of grinding and polishing for the preparation of steels for microstructural analyses. The shape of the waves at the interface is different for each plate

combination and it appears that the combinations with ferritic steel and TWIP steel show greater tendency for folds or distinct “hand-shakes” to occur, in contrast to the TWIP-TWIP combinations which produced a “peak and trough” interface.

For the regions examined in *Figures 5 to 12*, all plates showed good bonding by the EW process, apart from Plate 3 (*Figure 6*) in which debonding had occurred between the two TWIP steel plates of different thicknesses and this is clearly evidenced through cracking at the interface.

It was observed that regardless of the plate combinations used to produce each composite plate in this study, the interface microstructure was seen to possess a mixture of complex metallurgical features. These included severely-plastically deformed grains; solidified melts (zones which had melted and solidified during the welding processes as a result of high localised temperatures reached at the interface); associated solidification defects such as porosity or shrinkage cracks in the solidified melts; adiabatic shear band formation; as well as recrystallised grains. For further detailed information on microstructural characterisation at the interface of ferritic-martensitic and austenitic steels produced using the EW process, the reader is referred to the investigation undertaken in reference [1].

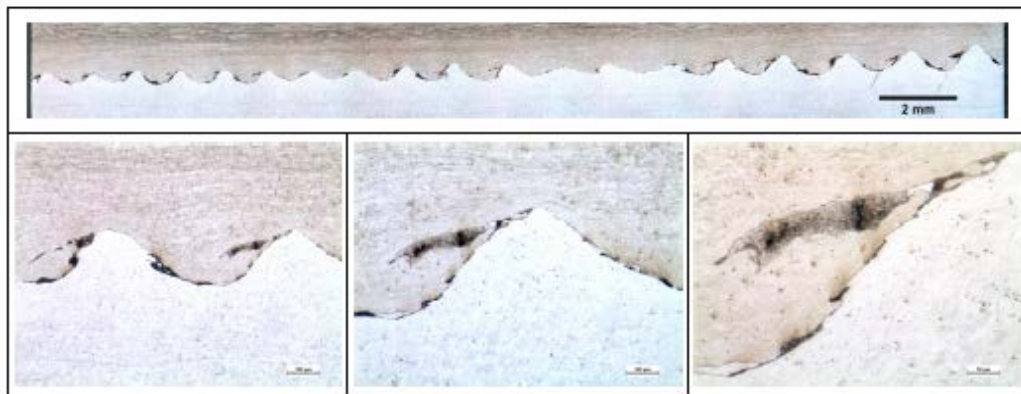


*Figure 5: Macrographs and micrograph of plate 1 TWIP (8.5) + TWIP (2.6). Top scale bar is 2 mm.*



*Figure 6: Macrographs and micrograph of plate 2 G350(8.5) + TWIP (2.6). Top scale bar is 2 mm.*

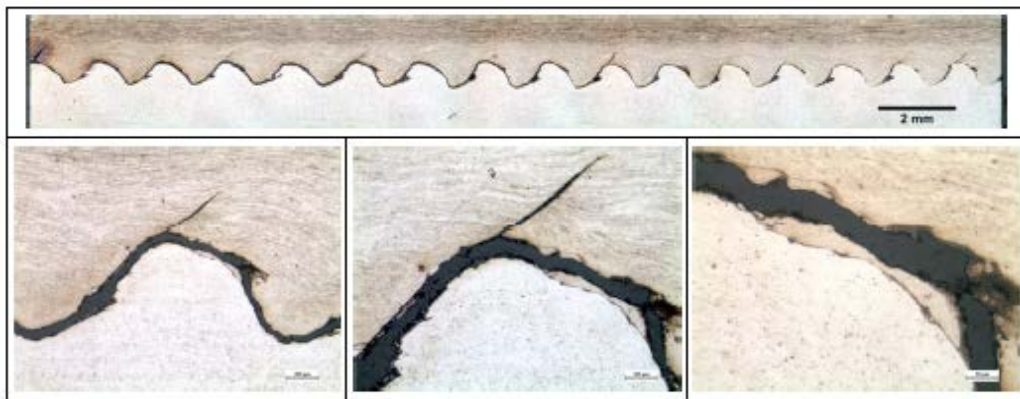


Figure 7: Macrographs and micrograph of plate 3 TWIP (2.6) + TWIP (8.5). Top scale bar is 2 mm.

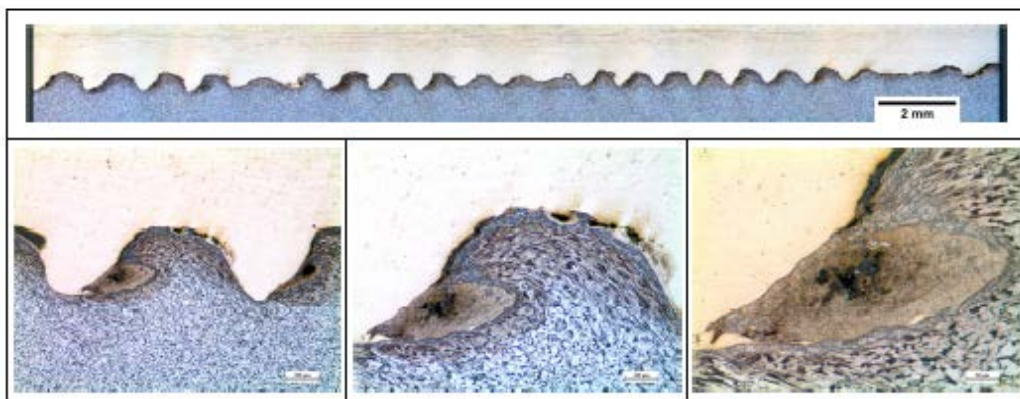


Figure 8: Macrographs and micrograph of plate 4 TWIP (2.6) + G350 (8.5). Top scale bar is 2 mm.

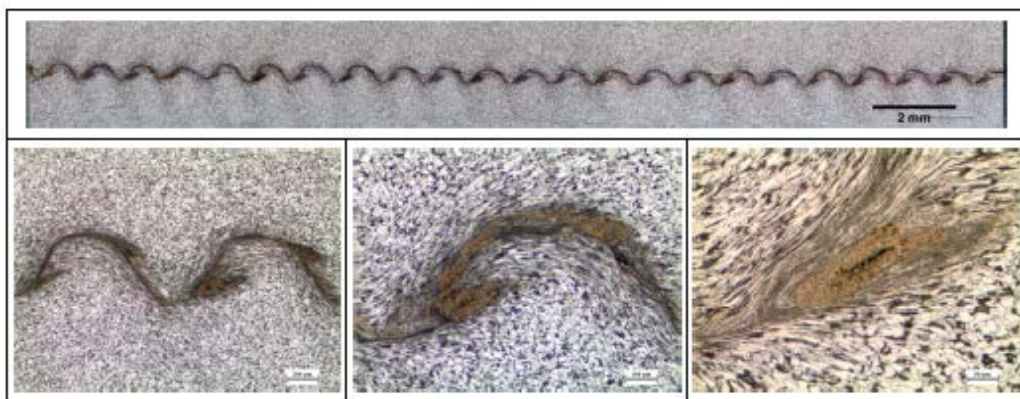


Figure 9: Macrographs and micrograph of plate 5 G350 (8.5) + G350 (8.5). Top scale bar is 2 mm.

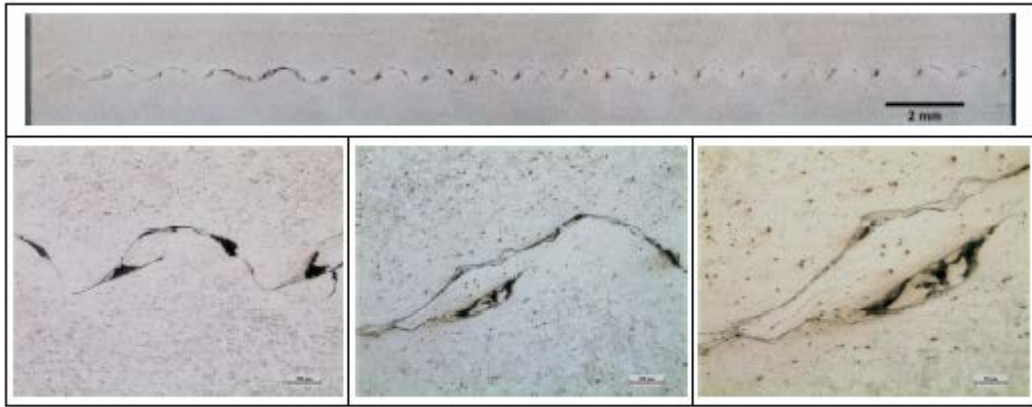


Figure 10: Macrographs and micrograph of plate 6 TWIP (8.5) + TWIP (8.5). Top scale bar is 2 mm.



Figure 11: Macrographs and micrograph of plate 7 TWIP (2.6) + TWIP (2.6). Top scale bar is 2 mm.

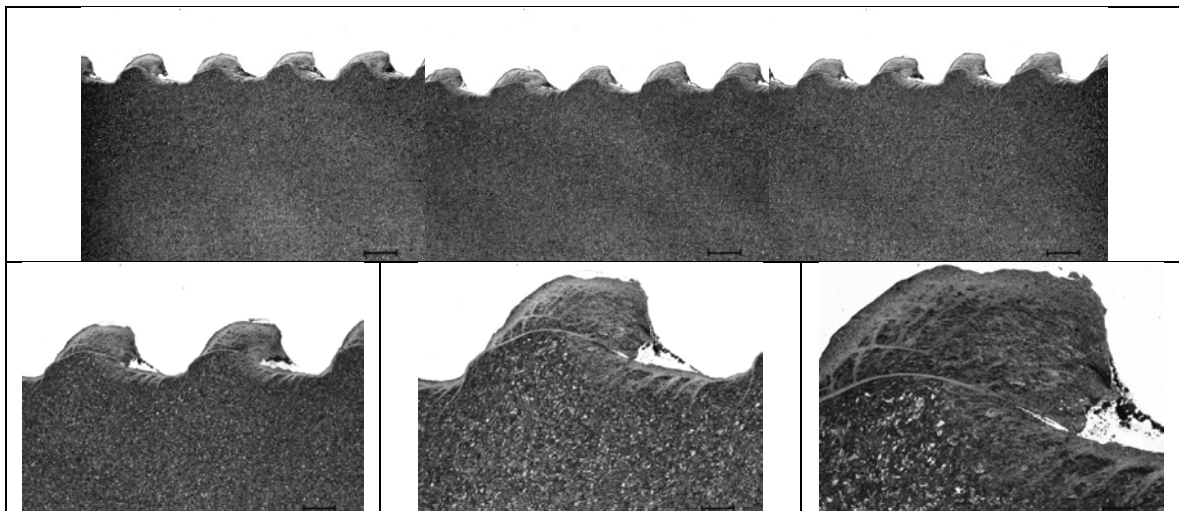


Figure 12: Macrographs and micrograph of plate 8 SA (8.5) + HARD (4.3) from adapted from [1]. Top scale bar is 380  $\mu$ m.

### 3.2 Residual Stress Development in Composite Plates

The development of residual stresses in the composite plate combinations, as a function of through-thickness position, is presented in *Figures 13 to 20*. There were a number of key observations, related to initial plate material combinations and plate thicknesses. It is important to note that the flyer plates location in *Figures 13 to 20* are always on the right hand side of each figure. The key observations for residual stress evolution in the composite plates are hence described as follows:

Regardless of plate material combinations, the longitudinal and transverse residual stresses showed very similar trends.

The maximum tensile stresses in both longitudinal and transverse directions were observed to occur in the vicinity of the weld interface in all combinations. This is due to the highly localised areas of intense deformation occurring at the weld interface, which causes heating during impact and on cooling, thermal shrinkage. This induces tensile residual stresses due to the misfits produced between the near weld-interface and the unaffected base metal. Further, as a result of these misfits and for equilibrium reasons, the unaffected base metal attains compressive stresses.

The tensile residual stresses were greatest for TWIP steel combinations, giving stresses of 600 MPa or greater at the weld interface. These values are similar to, or exceeding the yield strength of this material. The yield strengths of grade 350 and HARD steels were not exceeded. The yield strength of SA steel was slightly exceeded.

Mismatched plate thickness configurations generally possessed one plate with tensile surface residual stresses and the other plate with compression surface residual stresses. This is due to plasticity effects, where either compressive deformation occurred as a result of the explosion on the flyer plate, and/or due to bending occurring in the composite plate system as a result of the EW process.

Matched plate thickness configurations displayed a more conventional development of residual stresses through the thickness of the bi-metallic plate, with lower values of tensile or compressive surface stresses. These samples were generally less bent or warped in appearance as shown in *Figure 4*.

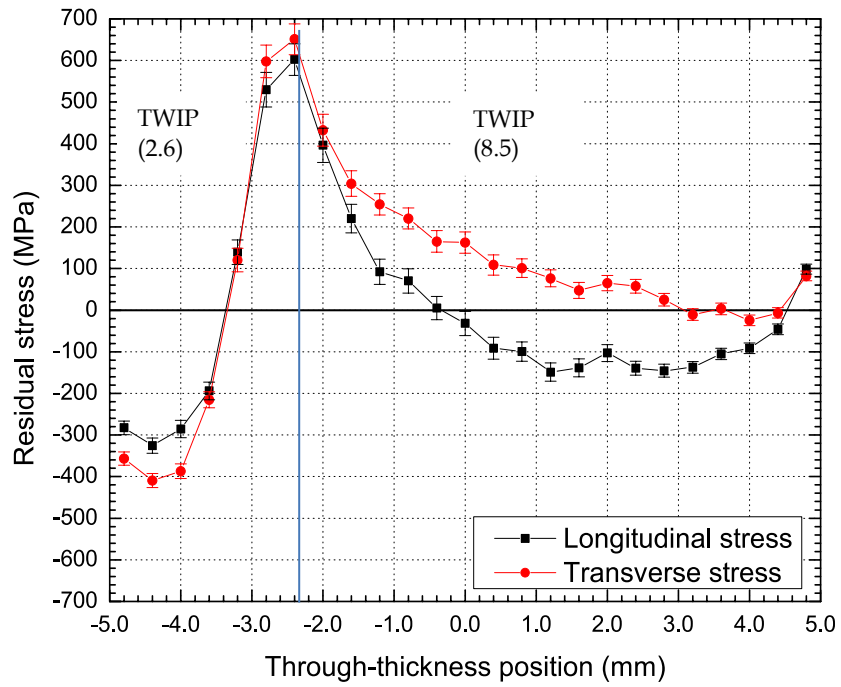


Figure 13: Longitudinal and transverse residual stresses in a composite plate 1 of TWIP (2.6) + TWIP (8.5).

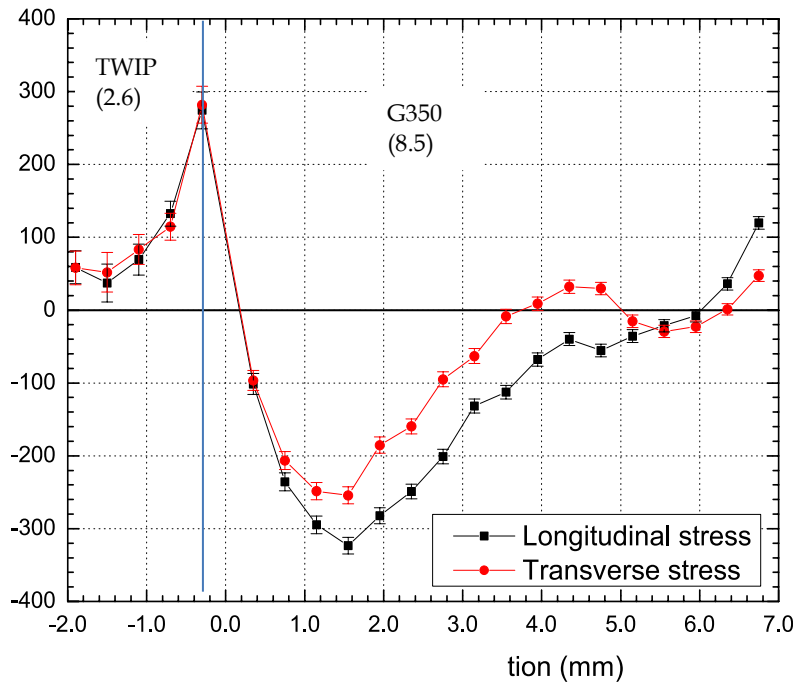


Figure 14: Longitudinal and transverse residual stresses in a composite plate 2 of TWIP (2.6) + G350(8.5).

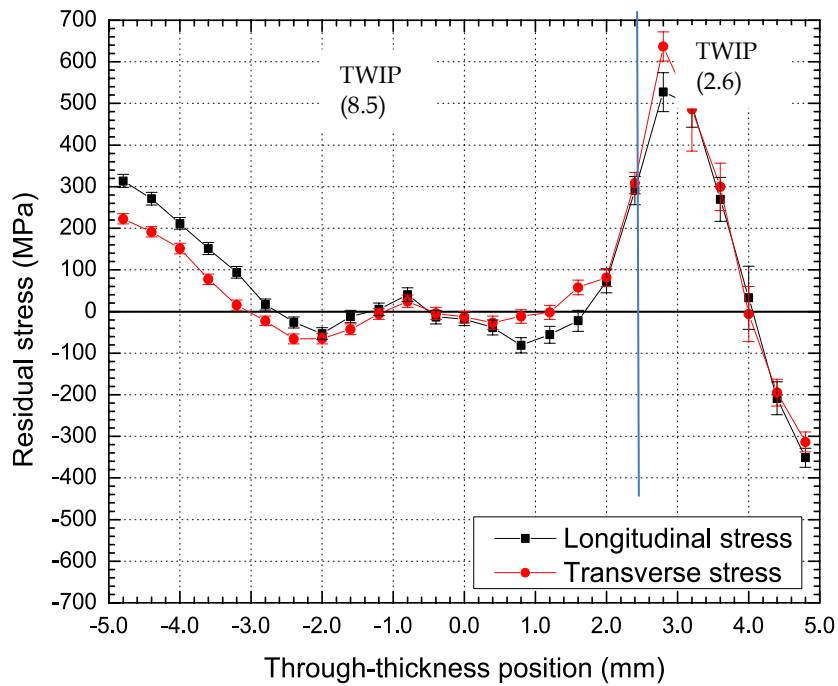


Figure 15: Longitudinal and transverse residual stresses in a composite plate 3 of TWIP (8.5) + TWIP (2.6).

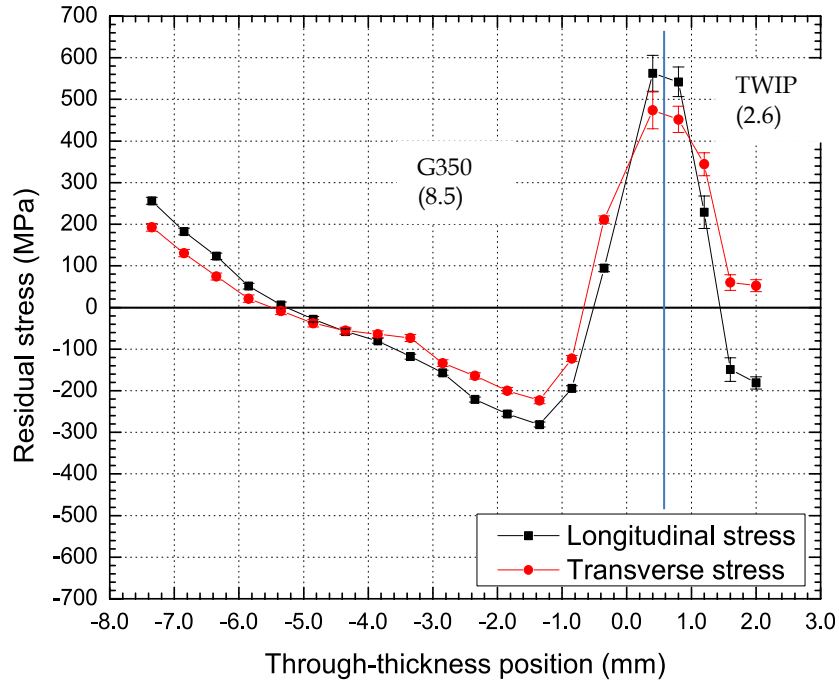


Figure 16: Longitudinal and transverse residual stresses in a composite plate 4 of G350 (8.5) + TWIP (2.6).

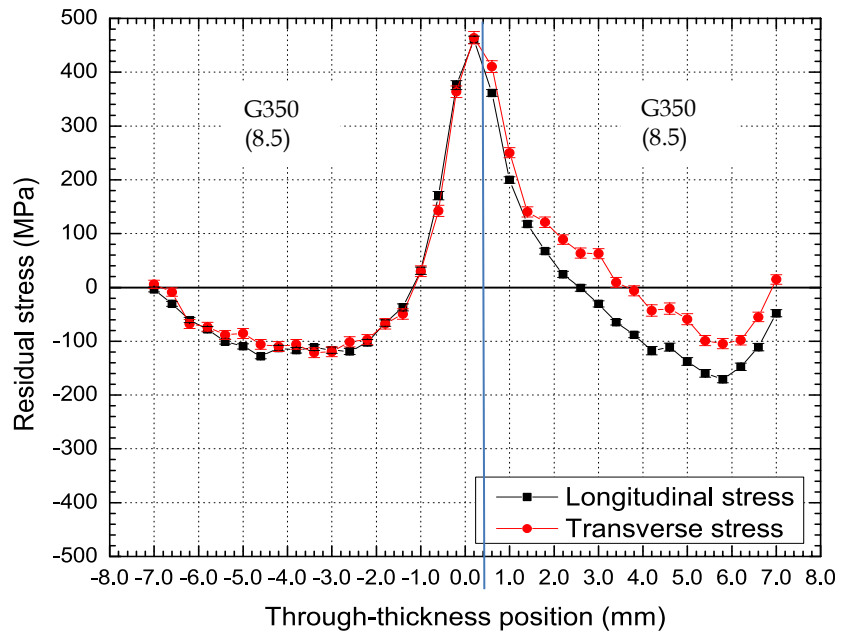


Figure 17: Longitudinal and transverse residual stresses in a composite plate 5 of G350 (8.5) + G350 (8.5).

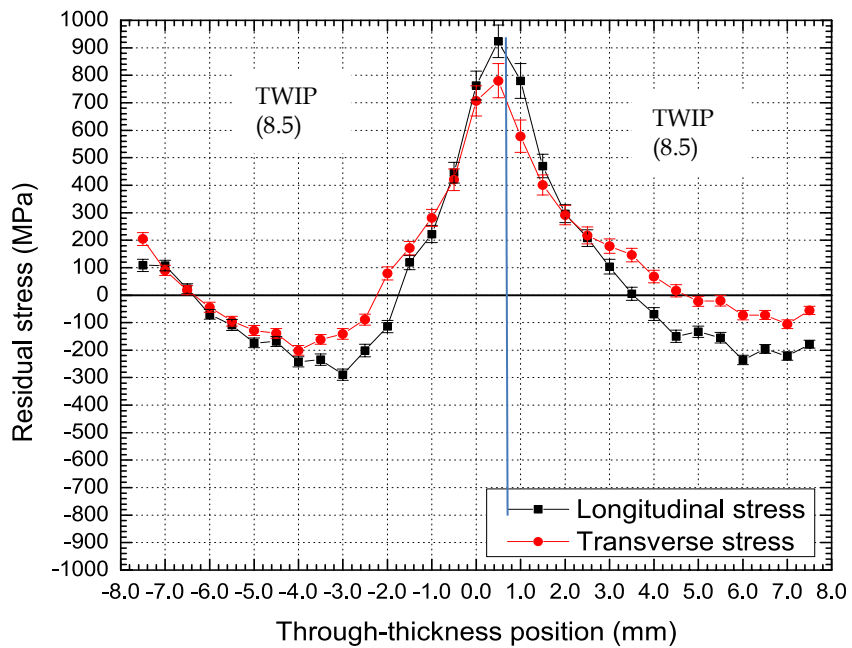


Figure 18: Longitudinal and transverse residual stresses in a composite plate 6 of TWIP (8.5) + TWIP (8.5).



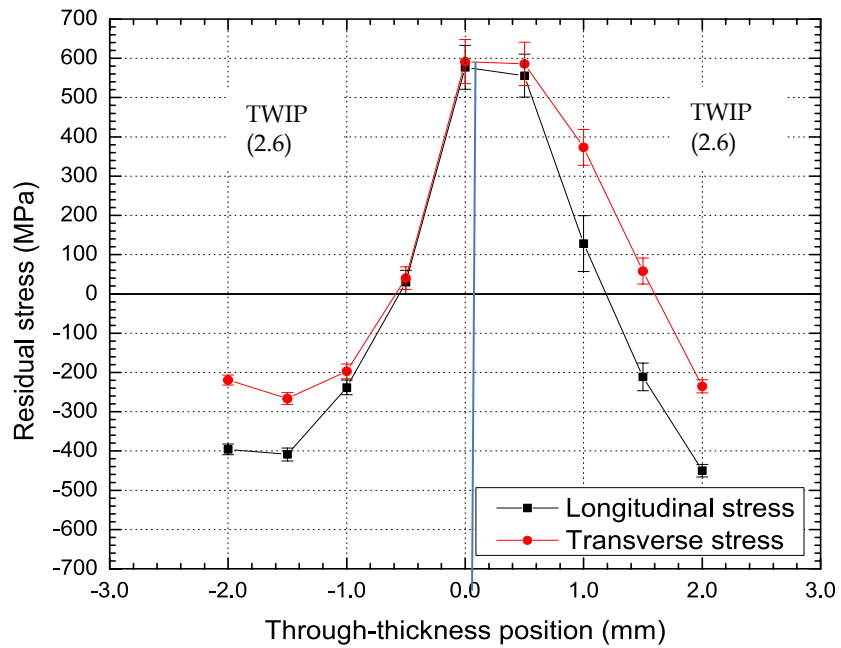


Figure 19: Longitudinal and transverse residual stresses in a composite plate 7 of TWIP (2.6) + TWIP (2.6).

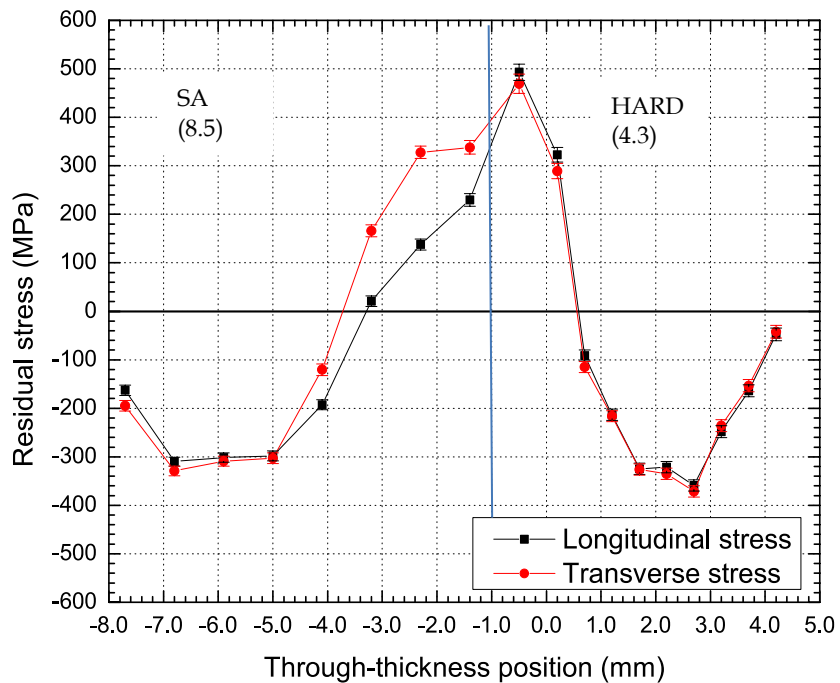


Figure 20: Longitudinal and transverse residual stresses in a composite plate 8 of SA (8.5) + HARD (4.3).

## 4. Conclusions

A series of eight bi-metallic composite plates were produced using the EW process, utilising a variety of steel plate chemistries, mechanical properties and plate thicknesses. Neutron residual stress measurements were undertaken to analyse the development of transverse and longitudinal residual stresses along the through-thickness direction of the bonded joints. Residual stress formation is dependent on welding processes, causing the formation of metallurgical features and plasticity at and near to the weld interface.

The trend of longitudinal and transverse residual stresses was essentially similar in all joints, regardless of materials combinations and thicknesses. Tensile residual stresses were found to be greatest at the weld interface, with compressive residual stresses produced in the unaffected base metal. The residual stresses present in TWIP steel and SA steel exceeded the yield strengths of these materials; however, yield strengths were not exceeded in either the grade 350 or HARD steels. Tensile and compressive surface residual stresses were observed in unmatched plate thickness combinations, with matched plate thickness combinations producing more uniform residual stress profiles.

The quantification of residual stress development in these systems may be used together with other analytical and mechanical techniques, to inform potential armour design based on composite plates produced through the EW process.

## 5. Acknowledgements

We gratefully acknowledge the assistance of Huijun Li for his valuable advice on Metallurgical subjects, Trevor Delaney for his hard work during the tests and Stewart Alkemade for his refereeing and correction of the paper.

## 6. References

- [1] C.-H. Choi, M.D. Callaghan, P. Van Der Schaaf, H. Li and B. Dixon, 'Modification of the Gurney equation for Explosive Bonding by Slanted Elevation Angle', Defence Science and Technology Organisation (DSTO), Technical Report 2013, pp. 1-46.
- [2] I. Tatsukawa, 'Residual Stress Measurements on Explosive Clad of Mild Steel', Trans. Japan Welding Soc., 39 (9), 1970, p951-957.
- [3] I. Tatsukawa, I. Oda, 'Residual Stress Measurements on Explosive Clad Stainless Steel', Trans. Japan Welding Soc., 2(2), 1971, p26-34.
- [4] R.V. Tamhankar and J. Ramesam, 'Metallography of Explosive Welds', Materials Science and Engineering, 13, 1974, p245-254.
- [5] C. Payares-Asprino, H. Katsumto, and S. Liu, 'Effect of Martensite Start and Finish Temperature on Residual Stress Development in Structural Steel Welds, Welding Journal, 87(11), 2008, p279-289.
- [6] G. V. Stepanov and S. G. Tsybochkin, 'Inelastic Deformation Of Sheet Blanks, In: Explosion Welding', Strength of Materials, 21 (9), 1987, p1249-1254.
- [7] R. Gurney, 'The Initial Velocities of Fragments From Bombs, Shells, and Grenades', Report No 405, Ballistic Research lab, Aberdeen, MD, Sep, 1943, AII-36218.

DEFENCE SCIENCE AND TECHNOLOGY ORGANISATION DOCUMENT CONTROL DATA				1. PRIVACY MARKING/CAVEAT (OF DOCUMENT)	
				2. TITLE  Residual Stress Development in Explosive-Bonded Bi-Metal Composite Materials	
4. AUTHOR(S)  C. Choi, V. Luzin, M. Callaghan, N. Lane and B. Dixon		5. CORPORATE AUTHOR  DSTO Defence Science and Technology Organisation 506 Lorimer St Fishermans Bend Victoria 3207 Australia			
6a. DSTO NUMBER DSTO-TR-2945	6b. AR NUMBER AR-015-876	6c. TYPE OF REPORT Technical Report	7. DOCUMENT DATE March 2014		
8. FILE NUMBER 2013-1112492/1	9. TASK NUMBER ARM 07/132	10. TASK SPONSOR	11. NO. OF PAGES 12	12. NO. OF REFERENCES 13	
13. DSTO Publications Repository  <a href="http://dspace.dsto.defence.gov.au/dspace/">http://dspace.dsto.defence.gov.au/dspace/</a>		14. RELEASE AUTHORITY  Chief, Land Division			
15. SECONDARY RELEASE STATEMENT OF THIS DOCUMENT  <i>Approved for Public Release</i>					
OVERSEAS ENQUIRIES OUTSIDE STATED LIMITATIONS SHOULD BE REFERRED THROUGH DOCUMENT EXCHANGE, PO BOX 1500, EDINBURGH, SA 5111					
16. DELIBERATE ANNOUNCEMENT  No Limitations					
17. CITATION IN OTHER DOCUMENTS Yes					
18. DSTO RESEARCH LIBRARY THESAURUS  blast, armour, bulge depth, comparison					
19. ABSTRACT  One of the main obstacles of applying explosive welding for improved mechanical and corrosion properties of the materials may be residual stress contour at the interface to be bonded, as this may be detrimental to the life of the vehicles. For this reason, it is important to study the distribution of the residual stress over the welded material, especially at the interface area.  Similar and dissimilar steel plate materials possessing different chemistries, mechanical properties and thicknesses, were explosive welded to successfully produce bi-metallic plates. Neutron diffraction experiments were undertaken to investigate the residual stress development in these bi-metallic plates. The characteristic residual stress formations in the plate systems were observed to be influenced by microstructural evolution at the weld interface as well as the mechanical properties and thicknesses of the original plate materials.  It was found that explosive welded plates have tensile residual stresses in both the longitudinal and transverse direction at the interface. The level of these stresses is close to yield.					